Length-Independent Charge Transport in Chimeric Molecular Wires

*Austin G. Wardrip[+], Amir Mazaheripour[+], Nina Hüsken, Jonah-Micah Jocson, Andrew Bartlett, Robert C. Lopez, Nathan Frey, Cade B. Markegard, Gregor Kladnik, Albano Cossaro, Luca Floreano, Alberto Verdini, Anthony M. Burke, Mary N. Dickson, Ioannis Kymissis, Dean Cvetko, Alberto Morgante, Sahar Sharifzadeh, Hung D. Nguyen, and Alon A. Gorodetsky**

Abstract: *Advanced molecular electronic components remain vital for the next generation of miniaturized integrated circuits. Thus, much research effort has been devoted to the discovery of lossless molecular wires, for which the charge transport rate or conductivity is not attenuated with length in the tunneling regime. Herein, we report the synthesis and electrochemical interrogation of DNA-like molecular wires. We determine that the rate of electron transfer through these constructs is independent of their length and propose a plausible mechanism to explain our findings. The reported approach holds relevance for the development of high-performance molecular electronic components and the fundamental study of charge transport phenomena in organic semiconductors.*

Molecular electronic devices have the potential to redefine integrated circuit technologies and revolutionize modern computing.[1,2] Consequently, much effort has focused on the discovery and study of nearly lossless molecular wires, that is, molecular chains that efficiently transport charge (notable π-conjugated examples include oligoporphyrins, oligophenylenevinylenes, and DNA).[3–8] Typically, such wires or bridges are electrically interrogated in various configurations, that is, scanning probe break junctions,[9,10] two terminal devices,[11,12] and self-assembled monolayers,[13,14] with the measurements yielding information on their ground state charge transport properties. However, for many of the reported molecular wires, the charge transport rate or conductivity drops off precipitously with length in the tunneling regime (typically $<$ ca. 5 nm).[9–18] Furthermore, artificial molecular wires are often difficult to synthesize, while natural molecular wires can exhibit poor stability under electrical interrogation.[9–18] Consequently, given the continued demand for integrated circuit miniaturization,[19] the development of high-performance molecular wires remains of paramount importance for next generation electronics.

Herein, we describe the preparation and characterization of bioinspired chimeric molecular wires. First, we design and synthesize a series of electroactive macromolecules from π-conjugated building blocks. Next, we self-assemble these constructs into monolayers and evaluate their orientations with X-ray spectroscopic techniques. Subsequently, we investigate the monolayers' electrochemical properties, and from these measurements, we extract the rate of electron transfer through the macromolecules, which we determine to be independent of their length. In turn, we use density functional theory (DFT) calculations to gain insight into the electronic structure of our constructs. Finally, we propose a plausible mechanism to explain our findings. The reported approach holds relevance for the development of high-performance molecular electronic components and the fundamental study of charge transport phenomena in organic semiconductors.

We began our experiments by drawing inspiration from the fields of organic electronics and oligonucleotide chemistry for the rational design and preparation of the macromolecules shown in Figure 1 A. First, we selected perylene-3,4,9,10 tetracarboxylic diimide (PTCDI) as the π-conjugated building block for our constructs because of this molecule's well-known electrochemical properties, propensity for adapting

[*] A. G. Wardrip,[+] R. C. Lopez, Prof. A. A. Gorodetsky
Department of Chemistry, University of California, Irvine
Irvine, CA 92697 (USA)
E-mail: alon.gorodetsky@uci.edu

A. Mazaheripour,[+] Dr. N. Hüsken, J.-M. Jocson, A. Bartlett, C. B. Markegard, Dr. A. M. Burke, M. N. Dickson, Prof. H. D. Nguyen, Prof. A. A. Gorodetsky
Department of Chemical Engineering and Materials Science
University of California, Irvine
Irvine, CA 92697 (USA)

N. Frey, Prof. S. Sharifzadeh
Department of Electrical and Computer Engineering
Boston University
Boston, MA 02215 (USA)

Dr. G. Kladnik, Dr. A. Cossaro, Dr. L. Floreano, Dr. A. Verdini, Prof. D. Cvetko, Prof. A. Morgante
CNR-IOM Laboratorio TASC
Trieste 34149 (Italy)

Dr. G. Kladnik, Prof. D. Cvetko
Faculty for Mathematics and Physics, University of Ljubljana
Jadranska 19, 1000 Ljubljana (Slovenia)

Prof. I. Kymissis
Department of Electrical Engineering, Columbia University
New York, NY 10027 (USA)

Prof. D. Cvetko
Institut J. Stefan
Jamova 39, 1000 Ljubljana (Slovenia)

Prof. A. Morgante
Department of Physics, University of Trieste
Trieste 34128 (Italy)

[+] These authors contributed equally to this work.

Supporting information for this article can be found under: http://dx.doi.org/10.1002/anie.201605411.

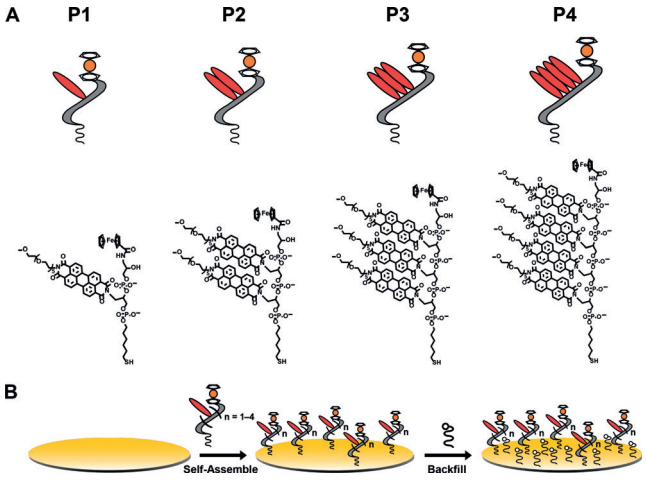

Figure 1. A) Illustration (top) and chemical structure (bottom) for macromolecules **P1**, **P2**, **P3**, and **P4**, which consist of tracts of one to four PTCDIs arranged on a phospho-alkane backbone and flanked by thiol-terminated linkers and ferrocene-terminated tethers. B) Illustration of self-assembled monolayer formation for the macromolecules in (A).

stacked columnar arrangements, and excellent stability under various conditions.[20,21] Next, we used standard automated oligonucleotide synthesis techniques, which are compatible with PTCDI derivatives,[22–27] to prepare, purify, and characterize thiol- and ferrocene-modified macromolecules featuring one, two, three, or four PTCDIs arranged on a phospho-alkane backbone (Supporting Information, Figures S1–16). Notably, our constructs' negatively-charged backbone and solubilizing hexaethylene glycol imide substituents facilitated processing and mitigated intermolecular aggregation. The final designer systems, which we denoted as **P1**, **P2**, **P3**, and **P4**, consisted of variable-length PTCDI tracts as the highly conductive components, terminal thiolated linkers as handles for monolayer formation, and pendant ferrocene moieties as redox probes of charge transport (Figure 1 A).

We proceeded to self-assemble and spectroscopically characterize monolayers from **P1**, **P2**, **P3**, and **P4**. As illustrated in Figure 1 B, we incubated clean gold substrates in solutions of each of our thiol-modified constructs, allowing for the formation of specific covalent S−Au bonds, and then treated the modified substrates with mercaptohexanol to enforce upright macromolecular orientations and displace non-specifically physisorbed species.[13,14,26,28–30] We subsequently confirmed the average orientations of the four monolayers' constituent macromolecules with near edge X-ray absorption fine structure spectroscopy (NEXAFS), which is a surface-sensitive technique that can elucidate the electronic characteristics and orientations of surface-confined molecules. Thus, we collected and analyzed partial electron yield spectra with the incident electric fields parallel and perpendicular to the surfaces of our substrates (Supporting Information, Figures S17–20).[31] Based on literature precedent for PTCDIs, we assigned the spectra's characteristic inequivalent doublets at energies between 284 and 286 eV to carbon 1s→π* transitions that are associated with these molecules' LUMO (left doublet) and LUMO + 1 (right doublet) (Supporting Information, Figures S18–21).[32] In turn, by evaluating the dependence of the LUMO + 1 signals' intensities on the polarization of the electric fields, we calculated average substrate-relative tilt angles of $61 \pm 2°$, $61 \pm 2°$, $60 \pm 2°$, and $60 \pm 2°$ for the constituent PTCDIs of monolayers from **P1**, **P2**, **P3**, and **P4**, respectively. Overall, the NEXAFS experiments indicated that our four macromolecules adopted nearly identical upright average orientations, in analogy to duplexes in backfilled DNA monolayers.[7,26,28–30]

We initially investigated the electrochemical properties of backfilled monolayers from **P0**, which is an analogue of our macromolecules but lacks any PTCDIs (Supporting Information, Figures S21 and S22 A). For these monolayers, we observed a redox couple at a potential of 0.46 ± 0.02 V versus Ag/AgCl, which we attributed to the pendant ferrocenes (Supporting Information, Figure S22 B).[13,14,33–35] The couple featured an anodic to cathodic peak current ratio of 1.07 ± 0.04, indicating a quasi-reversible redox reaction, and a linear dependence of the anodic peak current on the scan rate, indicating a surface-bound species (Supporting Information, Figure S22 C).[14,36] From the anodic wave, we calculated a surface coverage of 22.2 ± 4.3 pmol cm^{-2}, which was smaller than the estimated maximum coverages of circa 300 and circa 450 pmol cm^{-2} for ferrocene-terminated DNA and alkanethiol monolayers, respectively,[37,38] as well as a full width at half maximum (FWHM) of 0.14 ± 0.01 V, which was greater than the ideal value of approximately 0.091 V.[14,36] These metrics suggested relatively dilute monolayers, likely owing to the repulsive electrostatic interactions between our constructs' negatively-charged backbones.[14,36] Altogether, the measurements demonstrated that monolayers from **P0** generally resembled analogous monolayers from ferrocene-terminated alkanethiols.[13,14,33–35]

We next evaluated the rate of electron transfer between the pendant ferrocene redox probes and the gold surfaces for backfilled monolayers from **P0** (as mediated by the intervening phospho-alkane bridges). By analyzing the cyclic voltammograms obtained at different scan rates, we extracted the electron transfer rate constant k_0 according to the Laviron approach (Supporting Information, Figure S22 D).[14,39] The calculated rate constant for **P0** was $k_0 = 9.7 \pm 1 \times 10^2$ s^{-1} (corresponding to a probe-surface through-bond distance of 2.29 nm). This value was in good agreement with rate constants of 6.0×10^3, 1.2×10^3, and 1.0×10^2 s^{-1} reported for analogous ferrocene-terminated alkanethiol monolayers with probe-surface through-bond distances of 1.84, 2.00, and 2.47 nm, respectively (Table 1).[33–35] Our observations and analysis suggested that non-resonant tunneling was the likely mechanism governing electron transfer for **P0**.

We in turn investigated the electrochemical properties of backfilled monolayers from **P1**, **P2**, **P3**, and **P4** at positive potentials (Figure 2). These monolayers featured reversible redox couples at potentials from approximately 0.47 to approximately 0.52 V versus Ag/AgCl, anodic to cathodic peak current ratios of ca. 1.02 to ca. 1.16, anodic FWHMs of approximately 0.13 V, average surface coverages of ca. 20 pmol cm^{-2} to ca. 25 pmol cm^{-2}, and linear plots of peak current as a function of scan rate (Supporting Information, Figure S23 and Table S1). Altogether, our measurements

Table 1: Various ferrocene-terminated species, with the corresponding electron transfer rate constants k_0 and through-bond electron transfer distances.

Ferrocene Species	k_0 [s^{-1}]	Distance [nm][a]	Reference
$FcCONH(CH_2)_7SH$	6.6×10^4	1.53	34
$FcCONH(CH_2)_8SH$	1.5×10^4	1.69	34
$FcCONH(CH_2)_9SH$	6.0×10^3	1.84	34
$FcCONH(CH_2)_{10}SH$	1.2×10^3	2.00	34
$FcCO_2(CH_2)_{13}SH$	1.0×10^2	2.47	33
$Fc(CH_2)_{16}SH$	2.8×10^1	2.65	35
$FcCONH(CH_2)_{15}SH$	7.0×10^0	2.77	34
P0	$9.7\pm1\times10^2$	2.29	This work
P1	$8.2\pm1\times10^2$	3.05	This work
P2	$8.3\pm1\times10^2$	3.81	This work
P3	$8.8\pm1\times10^2$	4.57	This work
P4	$8.2\pm1\times10^2$	5.33	This work

[a] Electron transfer distance is defined as the sum of all the bond lengths between the pendant ferrocene and the terminal gold-bound sulfur atom.

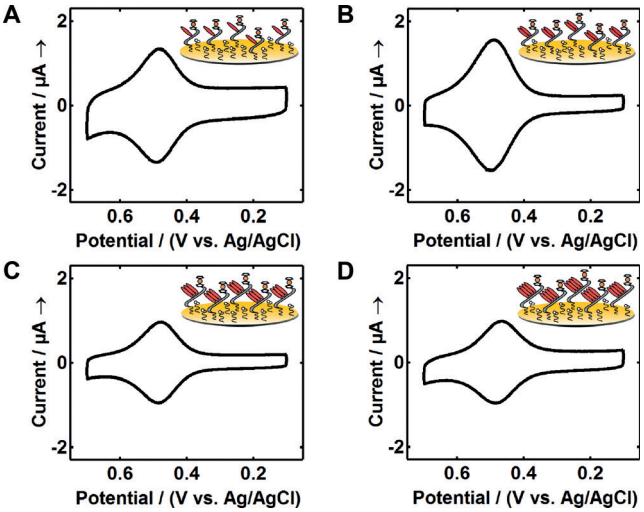

Figure 2. Cyclic voltammograms at positive potentials for backfilled monolayers from A) **P1**, B) **P2**, C) **P3**, and D) **P4**. The insets show schematics of the monolayers.

indicated that monolayers from **P1**, **P2**, **P3**, and **P4** were relatively dilute and that their electrochemical characteristics closely resembled not only those of **P0** but also each other.

We further explored the electrochemical properties of backfilled monolayers from **P1**, **P2**, **P3**, and **P4** at negative potentials (Supporting Information, Figure S24). We found one to three quasi-reversible redox couples for **P1**, **P2**, **P3**, and **P4**, with a midpoint potential of approximately −0.4 V versus Ag/AgCl for the initial (least negative) couple in each instance. Based on literature precedent for PTCDIs,[20,21,26] we attributed these redox signatures to the macromolecules' LUMOs (and energetically higher orbitals); and by using the pendant ferrocenes as internal standards,[36] we calculated reliable LUMO energies of -4.11 ± 0.01, -4.15 ± 0.01, -4.19 ± 0.01, and -4.22 ± 0.01 eV for **P1**, **P2**, **P3**, and **P4**, respectively. The lowering of the LUMO energies and appearance of multiple energetically similar states for the longer macromolecules indicated the likely presence of strong π–π stacking interactions between the constituent PTCDIs. Overall, the electrochemical measurements suggested that the macromolecules' PTCDI-based substructures essentially behaved as single electroactive units.

We next evaluated the rate of electron transfer through backfilled monolayers from **P1**, **P2**, **P3**, and **P4**. The PTCDI-based substructures, along with their terminal linkers and tethers, served as extended bridges that mediated electron transfer between the pendant ferrocene redox probes and the gold surfaces. By analyzing the cyclic voltammograms obtained at different scan rates for monolayers from **P1**, **P2**, **P3**, and **P4**, we extracted these macromolecules' respective electron transfer rate constants k_0.[14,39] Surprisingly, for **P1**, we found only a slight decrease in the electron transfer rate constant to $k_0 = 8.2\pm1\times10^2\ s^{-1}$ (relative to **P0**), despite **P1**'s larger probe-electrode through-bond distance of 3.05 nm (Table 1). The measured value was in stark contrast to the smaller rate constants of 2.8×10^1 and $7.0\times10^0\ s^{-1}$ found for ferrocene-terminated alkanethiols with probe-surface through-bond distances of 2.65 and 2.77 nm, respectively (Table 1).[33–35] Furthermore, we discovered that the rate constants remained almost unchanged for the longer macromolecules, with values of $k_0 = 8.3\pm1\times10^2\ s^{-1}$ for **P2**, $k_0 = 8.8\pm1\times10^2\ s^{-1}$ for **P3**, and $k_0 = 8.2\pm1\times10^2\ s^{-1}$ for **P4**, despite the substantially increased probe-surface through-bond distances of 3.81 nm for **P2**, 4.57 nm for **P3**, and 5.33 nm for **P4**, respectively (Table 1). Together, the measurements indicated that the rate of electron transfer through our molecular wires was effectively not attenuated with length.

To facilitate the interpretation of our experimental observations, we performed DFT calculations. We first adapted literature protocols[27] and used molecular dynamics (MD) simulations to obtain the lowest free energy (most thermodynamically stable) atomistic conformations for the PTCDI-based substructures of **P1**, **P2**, **P3**, and **P4** (Supporting Information, Figures S25 and S26). The simulations revealed that the constituent PTCDIs of **P2**, **P3**, and **P4** were offset with respect to one another but still featured strong π–π stacking interactions, in agreement with the characteristic changes observed for the constructs' UV/Vis spectra (Supporting Information, Figures S14–16). Next, we employed the simulated equilibrium geometries and the long-range-corrected CAM-B3LYP functional[40] to generate the shapes and energies of our four macromolecules' HOMOs and LUMOs. The isosurface plots revealed that the electron density was delocalized over either the entirety or majority of the substructures' aromatic cores, demonstrating that their constituent PTCDI moieties were not electronically independent of each other (Supporting Information, Figure S27). Moreover, the theoretically-predicted LUMO energies were lowered for the longer macromolecules, with values of −2.66, −3.01, −3.36, and −3.36 eV for **P1**, **P2**, **P3**, and **P4**, respectively, in agreement with the trend found for the electrochemical measurements (note that the theoretical and experimental values did not perfectly match owing to the limited accuracy of the functional and the exclusion of solvent and/or substrate effects). Overall, the calculations gave insight into the electronic structures of our constructs and

provided a rationale for their electrochemical behavior as single electroactive units.

Our experimental findings warrant a discussion of the mechanisms governing charge transport for **P1**, **P2**, **P3**, and **P4**. We note that our constructs consist of the following distinct components: π-conjugated PTCDI-based substructures, primarily saturated tethers bound to the gold surfaces, and primarily saturated linkers connected to the pendant ferrocene probes (Figure 1 A). Based on previous findings for ferrocene-terminated alkanethiols[13,14,33–35] (as well as our experimental observations for monolayers from **P0**), electrons are likely transported through the macromolecules' tethers and linkers by a rate-limiting and lossy non-resonant tunneling mechanism.[2,13–18] Furthermore, based on reports of rapid electron hopping rates of $> 10^7\ s^{-1}$ [25] and femtosecond charge transfer times[41] in analogous PTCDI-based ensembles (as well as our computational observations for **P1**, **P2**, **P3**, and **P4**), electrons are likely transported through the macromolecules' PTCDI-based substructures by a rapid and nearly lossless resonant tunneling mechanism.[2,13–18] The combination of these two mechanisms accounts for the observation of essentially length-independent charge transport for our constructs.

In summary, we have synthesized a series of bioinspired chimeric molecular wires and electrochemically characterized their charge transport properties. Our study holds significance for several reasons. First, the reported synthetic methodology employs straightforward, readily accessible bioconjugate chemistry techniques to prepare well-defined PTCDI-based macromolecules. In principle, this approach possesses few limitations and could be used to prepare a variety of modular, sequence-variable constructs from arbitrary organic semiconductor building blocks. Second, our electrochemical strategy makes it possible to simultaneously measure electron transfer rates and monitor changes in electronic structure. Such experimental flexibility underscores the value of our methodology for the study of nanoscale charge transport phenomena. Finally, the measurements reveal that charge transport through our molecular wires is essentially independent of length. The reported constructs may thus prove valuable as archetypes for the construction of novel high-performance electronic components. Altogether, our findings hold broad relevance within the context of molecular, organic, and biological electronics and may afford new opportunities for the development of advanced miniaturized circuits.

Acknowledgements

A.A.G. was supported by the Air Force Office of Scientific Research (FA9550-13-1-0096). The MD studies used resources supported by the National Science Foundation (OCI-1053575 and CHE-0840513). The DFT studies used resources at the National Energy Research Scientific Computing Center, which is supported by the Department of Energy (DE-AC02-05CH11231). D.C. and G.K. acknowledge partial financial support from the Javna Agencija za Raziskovalno Dejavnost RS (program P1-0112 and project Z1-6726). D.C. also acknowledges partial financial support from the Consiglio Nazionale delle Ricerche (CNR-STM 2014 program). The synchrotron experiments were performed at the ALOISA beam line of the IOM-CNR Laboratory at the Elettra synchrotron light source and were supported by the Ministero dell'Istruzione, dell'Università e della Ricerca (PRIN 20105ZZTSE) and the Ministero degli Affari Esteri e della Cooperazione Internazionale (US14GR12).

Keywords: bioinspired materials · charge transport · electrochemistry · molecular wires · organic electronics

How to cite: *Angew. Chem. Int. Ed.* **2016**, *55*, 14267 – 14271
Angew. Chem. **2016**, *128*, 14479 – 14483

[1] *Handbook of Single-Molecule Electronics* (Ed. K. Moth-Poulsen), Pan Stanford Publishing, Boca Raton, **2015**.
[2] *Charge and Exciton Transport Through Molecular Wires* (Eds. L. D. A. Siebbeles, F. C. Grozema), Wiley-VCH, Weinheim, **2011**.
[3] G. Sedghi, V. M. García-Suárez, L. J. Esdaile, H. L. Anderson, C. J. Lambert, S. Martín, D. Bethell, S. J. Higgins, M. Elliot, N. Bennett, J. E. Macdonald, R. J. Nichols, *Nat. Nanotechnol.* **2011**, *6*, 517 – 523.
[4] G. Sedghi, L. J. Esdaile, H. L. Anderson, S. Martin, D. Bethell, S. J. Higgins, R. J. Nichols, *Adv. Mater.* **2012**, *24*, 653 – 657.
[5] W. B. Davis, W. A. Svec, M. A. Ratner, M. R. Wasielewski, *Nature* **1998**, *396*, 60 – 63.
[6] H. D. Sikes, J. F. Smalley, S. P. Dudek, A. R. Cook, M. D. Newton, C. E. D. Chidsey, S. W. Feldburg, *Science* **2001**, *291*, 1519 – 1523.
[7] J. D. Slinker, N. B. Muren, S. E. Renfrew, J. K. Barton, *Nat. Chem.* **2011**, *3*, 228 – 233.
[8] L. Xiang, J. L. Palma, C. Bruot, V. Mujica, M. A. Ratner, N. Tao, *Nat. Chem.* **2015**, *11*, 221 – 226.
[9] N. J. Tao, *Nat. Nanotechnol.* **2006**, *1*, 173 – 181.
[10] S. V. Aradhya, L. Venkataraman, *Nat. Nanotechnol.* **2013**, *8*, 399 – 410.
[11] C. Jia, B. Ma, N. Xin, X. Guo, *Acc. Chem. Res.* **2015**, *48*, 2565 – 2575.
[12] H. Song, M. A. Reed, T. Lee, *Adv. Mater.* **2011**, *23*, 1583 – 1608.
[13] M. D. Newton, J. F. Smalley, *Phys. Chem. Chem. Phys.* **2007**, *9*, 555 – 572.
[14] A. L. Eckermann, D. J. Field, J. A. Shaw, T. J. Meade, *Coord. Chem. Rev.* **2010**, *254*, 1769 – 1802.
[15] E. A. Weiss, M. R. Wasielewski, M. A. Ratner, *Top. Curr. Chem.* **2005**, *257*, 103 – 133.
[16] C. Schubert, J. T. Margraf, T. Clark, D. M. Guldi, *Chem. Soc. Rev.* **2015**, *44*, 988 – 998.
[17] S. S. Skourtis, *Biopolymers* **2013**, *100*, 82 – 92.
[18] R. J. Nichols, S. J. Higgins, *Annu. Rev. Anal. Chem.* **2015**, *8*, 389 – 417.
[19] M. M. Waldrop, *Nature* **2016**, *530*, 144 – 147.
[20] F. Würthner, *Chem. Commun.* **2004**, 1564 – 1579.
[21] C. Huang, S. Barlow, S. R. Marder, *J. Org. Chem.* **2011**, *76*, 2386 – 2407.
[22] C. Wagner, H.-A. Wagenknecht, *Org. Lett.* **2006**, *8*, 4191 – 4194.
[23] D. Baumstark, H.-A. Wagenknecht, *Chem. Eur. J.* **2008**, *14*, 6640 – 6645.
[24] T. A. Zeidan, R. Carmieli, R. F. Kelley, T. M. Wilson, F. D. Lewis, M. R. Wasielewski, *J. Am. Chem. Soc.* **2008**, *130*, 13945 – 13955.
[25] T. M. Wilson, T. A. Zeidan, M. Hariharan, F. D. Lewis, M. R. Wasielewski, *Angew. Chem. Int. Ed.* **2010**, *49*, 2385 – 2388; *Angew. Chem.* **2010**, *122*, 2435 – 2438.

[26] C. H. Wohlgamuth, M. A. McWilliams, A. Mazaheripour, A. M. Burke, K.-Y. Lin, L. Doan, J. D. Slinker, A. A. Gorodetsky, *J. Phys. Chem. C* **2014**, *118*, 29084 – 29090.
[27] C. B. Markegard, A. Mazaheripour, J.-M. Jocson, A. M. Burke, M. N. Dickson, A. A. Gorodetsky, H. D. Nguyen, *J. Phys. Chem. B* **2015**, *119*, 11459 – 11465.
[28] R. Levicky, T. M. Herne, M. J. Tarlov, S. K. Satija, *J. Am. Chem. Soc.* **1998**, *120*, 9787 – 9792.
[29] A. Anne, C. Demaille, *J. Am. Chem. Soc.* **2006**, *128*, 542 – 557.
[30] A. A. Gorodetsky, M. C. Buzzeo, J. K. Barton, *Bioconjugate Chem.* **2008**, *19*, 2285 – 2296.
[31] J. Stöhr, *NEXAFS Spectroscopy*, Springer-Verlag, Berlin/Heidelberg, Germany, **1992**.
[32] G. Fratesi, V. Lanzilotto, S. Stranges, M. Alagia, G. P. Brivio, L. Floreano, *Phys. Chem. Chem. Phys.* **2014**, *16*, 14834 – 12296.
[33] D. B. Robinson, C. E. D. Chidsey, *J. Phys. Chem. B* **2002**, *106*, 10706 – 10713.
[34] K. Weber, L. Hockett, S. Creager, *J. Phys. Chem. B* **1997**, *101*, 8286 – 8291.
[35] J. F. Smalley, H. O. Finklea, C. E. D. Chidsey, M. R. Linford, S. E. Creager, J. P. Ferraris, K. Chalfant, T. Zawodzinsk, S. W. Feldberg, M. D. Newton, *J. Am. Chem. Soc.* **2003**, *125*, 2004 – 2013.
[36] A. J. Bard, L. R. Faulkner, *Electrochemical Methods: Fundamentals and Applications*, 2nd ed., John Wiley and Sons, New York, **2000**.
[37] R. C. Mucic, M. K. Herrlein, C. A. Mirkin, R. L. Letsinger, *Chem. Commun.* **1996**, 555 – 557.
[38] C. E. D. Chidsey, C. R. Bertozzi, T. M. Putvinski, A. M. Mujsce, *J. Am. Chem. Soc.* **1990**, *112*, 4301 – 4306.
[39] E. Laviron, *J. Electroanal. Chem.* **1979**, *101*, 19 – 28.
[40] T. Yanai, D. P. Tew, N. C. Handy, *Chem. Phys. Lett.* **2004**, *393*, 51 – 57.
[41] A. Mazaheripour, G. Kladnik, J.-M. Jocson, A. G. Wardrip, C. B. Markegard, N. Frey, A. Cossaro, L. Floreano, A. Verdini, A. Bartlett, A. M. Burke, N. Hüsken, K. Miller, K. Van Wonterghem, R. Lopez, M. Lu, A. Masurkar, M. N. Dickson, S. Sharifzadeh, H. D. Nguyen, I. Kymissis, D. Cvetko, A. Morgante, A. A. Gorodetsky, submitted.

Received: June 3, 2016
Revised: July 14, 2016
Published online: October 7, 2016